BioOne COMPLETE

Mapping Potential Areas for Conservation Under Forest Carbon Credit Eligibility in a Natural Protected Area in Northern Mexico

Authors: Orta-Salazar, Carolina, Aguirre-Salado, Carlos Arturo, Reyes-Hernández, Humberto, Reyes-Agüero, Juan Antonio, and Muñoz-Robles, Carlos Alfonso

Mapping Potential Areas for Conservation Under Forest Carbon Credit Eligibility in a Natural Protected Area in Northern Mexico

Carolina Orta-Salazar[1], Carlos Arturo Aguirre-Salado[2] ⓘ,
Humberto Reyes-Hernández[1,3], Juan Antonio Reyes-Agüero[1,4],
and Carlos Alfonso Muñoz-Robles[1,4]

Abstract
Emerging carbon markets are posing new challenges for stakeholders. In order to operationalize the selection of feasible areas to promote above-ground carbon capture and quantify its potential as claimed in the norm NMX-AA-173-SCFI-2015, a methodology may be proposed. Above-ground tree biomass geospatial estimates at the pixel level, neighboring land cover, and legal information were combined in order to obtain the potential for above-ground carbon capture. Forest above-ground tree carbon capture estimates were conducted under the assumption that forest cover in bare soil land will be recovered to the most conserved neighboring vegetation type. This approach may be used in other situations around the world where potential carbon estimates are required to design forest carbon capture projects considering native vegetation type.

Introduction

According to the last official communication related to the National Greenhouse Inventory in Mexico, during the 1990–2012 period, carbon capture potential achieved by forest recovery in the whole country was estimated as 12 Mt CO_2 (INECC/SEMARNAT, 2015). In 2015, the Mexican Official Standard (MOS) to register forest carbon projects and certify the increase in carbon stocks (NMX-AA-173-SCFI-2015) was published (Ministry of Economy, 2015). This regulation is focused on implementing projects for capturing forest carbon in degraded/abandoned/nonforested lands using a base line as reference.

In accordance with the Mexican standard, Principle 1 states that, in the Criterium 1.3., forest carbon capture projects must be carried out on lands where participants can demonstrate land ownership and carbon sequestration rights, *i.e.*, accreditation of legal land tenure; consequently, there should be evidence that the land ownership rights will not lead to conflict either with those in the community or between different

neighbouring comunities or ejidos. Criterium 1.4. states that the project must fulfill all applicable regulations, including to show, as part of the documentation, the existence of a) current forest management program, b) reports concerning the advance of the forest management program on a year-by-year basis, and c) the revision of the National Agrarian Registry to ensure the lack of conflicts over land rights. While in Principle 5,

[1]Programa Multidisciplinario de Posgrado en Ciencias Ambientales, Universidad Autónoma de San Luis Potosí, Mexico
[2]Facultad de Ingeniería, Universidad Autónoma de San Luis Potosí, Mexico
[3]Facultad de Ciencias Sociales y Humanidades, Universidad Autónoma de San Luis Potosí, Mexico
[4]Instituto de Investigación de Zonas Desérticas, Universidad Autónoma de San Luis Potosí, Mexico

Corresponding Author:
Carlos Arturo Aguirre-Salado, Universidad Autónoma de San Luis Potosí, 78280, Manuel Nava 8, Zona Universitaria, San Luis Potosí, México.
Email: carlos.aguirre@uaslp.mx

Criterium 5.7 states that the internal governance processes of the ejidos and local communities and other project participants as well as their rights, uses, and customs must be respected during the project's design and implementation, which can also be verifiable by ensuring that the land tenure is free from conflict; further, Criterium 5.11 states that there should be participatory and representative forums or periodic assemblies, where the design, execution, and follow-up of the projects are discussed and analyzed to address comments or conflicts that may arise during the life of the project, which can be verifiable by evidence such as meeting acts that demonstrate the analysis or discussion of the forest carbon capture project conducted by participants in the community or ejido (Ministry of Economy, 2015).

However, additional criteria apply for a land to be eligible for a forest carbon capture project. There are geospatial requirements, for example, that need to be addressed to implement the MOS for a specific land base, which may be summarized in 1) areas with no forests, 2) in a certain successional vegetation stage, and 3) in a forest density condition less than 25% over the last five years. Although the MOS suggests the following six eligible activities for capturing forest carbon (*i.e.*, reforestation, forestation, forest regeneration, sustainable forest management, forest conservation, and agroforestry), this methodological approach only can be applied for the former three forestry activities related to forest restoration. After five years of the existence of the Mexican government's standard (*i.e.*, MOS), to our knowledge, no forest carbon projects have been registered under the new regulation.

In order to assess an ecosystem's capacity to capture forest carbon, remote sensing plays a key role in estimating above-ground tree biomass by combining a series of techniques that may include forest inventory, digital processing of remotely sensed spectral data, and the use of estimation/classification algorithms to find relationships between the field and spectral data (Ruiz et al., 2014). Several approaches have been taken for estimating biomass/carbon at different spatial and temporal scales. Spatial scales include the global, country, or regional level and a finer local level. At the global level, several authors conducted spatially explicit biomass/carbon estimations with coarse spatial resolution remotely sensed data, *i.e.*, MODIS. Algorithms used in this context include the 6S radiative transfer algorithm, vegetation change tracker algorithm (VCT) (Kim et al., 2014), MODIS tree cover VCF, training data automation and support vector machines (TDA-SVM) (Sexton et al., 2013). At the country/regional level, other authors conducted spatially explicit biomass estimations with medium spatial resolution remotely sensed data, *i.e.*, Landsat and SPOT. Algorithms used in this context include linear and exponential models (Anaya et al., 2009; Nelson et al.,

2017), random forests (Cartus et al., 2014; Thomas et al., 2019), classification and regression trees (Chubey et al., 2006), posterior probability of membership (Gallaun et al., 2010), multiscale spectral-spatial-temporal super-resolution mapping (Zhang et al., 2017), and stochastic gradient boosting (Freeman et al., 2016). At the local level, some authors performed spatially explicit biomass estimations with high spatial resolution remotely sensed data, *i.e.*, Ikonos, Quickbird, Geoeye, Worldview. Algorithms used in this context include *k*-nearest-neighbor (kNN) (Breidenbach et al., 2012; Sun et al., 2015), linear regression modeling (Neigh et al., 2016), and linear regression following Fourier-based textural ordination (Proisy et al., 2007).

On the temporal domain, remotely sensed data-based biomass/carbon studies can be classified into three groups: 1) single-date studies for biomass/carbon variable retrieval based on continous (estimation), as tasseled cap distance (TCD) (Gómez et al., 2011), random forest (RF), and the maximum entropy (ME) algorithms (Xu et al., 2016); 2) multitemporal studies *i.e.*, from two to five dates of analysis for monitoring land use/biomass dynamic time warping (DTW) (Gómez et al., 2014); and 3) hypertemporal studies for monitoring biomass in time series, *e.g.*, iterative reweighted multivariate alteration detection (IR-MAD) process (Gómez et al., 2012), LandTrendr (Landsat-based detection of trends in disturbance and recovery), image trends from regression analysis (ITRA), vegetation change tracker (VCT), exponentially weighted moving average change detection (EWMACD), multi-index integrated change analysis (MIICA), Continuous Change Detection and Classification (CCDC), and vegetation regeneration and disturbance estimates through time (VeRDET) (Cohen et al., 2017).

Despite the existence of multiple remotely sensed spectral data based studies for monitoring biomass/carbon at different spatial and temporal scales, their direct application to the MOS is still difficult. These approaches have not been designed specifically to implement the Mexican standard itself but to satisfy different information requirements in their application countries. Thus, the objective of this work is to propose a methodological framework by identifying those specific sites for capturing above-ground tree carbon that fulfill the criteria established in the MOS (NMX-AA-173-SCFI-2015) and quantifying the theoretical potential amount of above-ground tree carbon capture.

Methods

Study Site

The study area is located at the Priority Region for Conservation Xilitla (PRCX), San Luis Potosí, Mexico. This is a natural protected area officially

decreed since 1923 as "National Forest Reserve Xilitla Wooded Portion." The area is located at the southeast portion of the state of San Luis Potosí, in the Huasteca Potosina region in Mexico, mainly covering the municipality of Xilitla and some parts of the municipality of Aquismón (Figure 1). The study area has temperate and dense forests characterized by the genus *Pinus spp.*, *Quercus spp.*, *Abies sp.*, and *Liquidambar sp.* (De Jong et al., 2010; Reyes et al., 2016).

Landsat is a satellite mission that offers a free-of-charge, high-quality, and vast amount of spectral information of Earth on a nearly permanent basis at high spatial resolution. The Landsat platform was selected as the primary data source because of the full coverage of the entire land surface, which makes it possible to monitor land cover change across landscapes at regional and local scales. Two Landsat scenes located at path: 026/row: 045 were downloaded from the USGS GloVis platform available at https://glovis.usgs.gov/. The first image was taken by Landsat 5 TM on April 13, 2011, at 16:48 h (LT05_L1TP_026045_20110413_20161208_01_T1). Sun elevation and sun azimuth were 61.71° and 112.29°, respectively. The second one was taken by Landsat 8 OLI on April 29, 2017, at 16:58 h (LC08_L1TP_026045_20170429_20180125_01_T1). Sun elevation and sun azimuth were 66.97° and 103.78°, respectively (Figure 2A to C). Landsat imagery was pre-processed by applying an absolute correction. Digital numbers were converted to top-of atmosphere (TOA) reflectance (Young et al., 2017). For the case of Landsat 5 TM, all spectral bands were used, except for the thermal band; for the case of Landsat 8 OLI, only bands 1 through 7 were considered. Topographic normalization was applied to both Landsat images by using the C-correction algorithm in order to minimize the effects of mountainous terrain on reflectance (Teferi et al., 2010). Atmospheric correction was not applied to imagery because 1) it was cloud-free within the study area, and aerosols were accounted as neglected, and 2) the change-detection method selected was post-classification, that is, each image was classified individually and then compared for change analysis, *i.e.*, spectral documentation of training fields was created over each Landsat scene in a separate method; further any inter-scene radiometric effect was also considered as inappreciable (Edwards, 1998; Paolini et al., 2006).

To bolster the spectral and spatial variability of vegetation cover and to facilitate the training field selection, false color composites were built using different band combinations. For the case of Landsat 5 TM, the band combination employed was as follows: blue for band 3 (red), green for band 4 (near infrared), red for band 5 (shortwave infrared 1). While for the case of Landsat 8 OLI, the band combination was as follows: blue for band 4 (red), green for band 5 (near infrared), red for
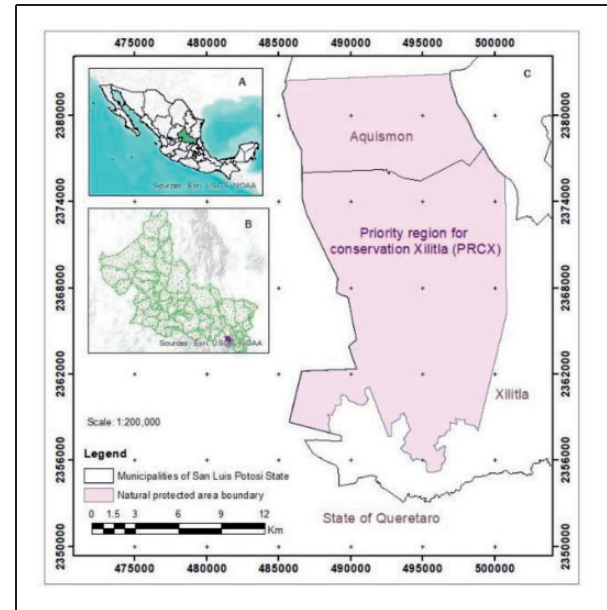

Figure 1. Study area. A: Map of Mexico; B: Map of the State of San Luis Potosi and C: Priority Region for Conservation Xilitla (PRCX).

band 6 (shortwave infrared 1). One criterium to select areas than can be eligible to apply the new MOS is that the site has been with no forest, at least during the previous five years, with respect to the elaboration of the proposal. To identify such fullfilment, a forest/nonforest map was created by applying a *k*-nearest-neighbor algorithm (*k*NN) to the two satellite images (McRoberts, 2008).

Since, in this part of the methodology, it was only required to differentiate between forested and nonforested land, it was not considered necessary to know the vegetation type as an outcome from processing remotely sensed data; thus, only four thematic classes associated with forested land were identified by photo-interpretation, regardless of their vegetation type. Accordingly, in order to identify bare soil during the last five years, it was necessary to create a map of only two thematic classes: forested and nonforested. Conducting a single classification with the only two thematic classes required would have created spectral signatures with a broad range of radiometric values, making fine classification of pixels difficult. Therefore, to minimize the variability of data used as training fields for the creation of each spectral signature and to encompass the whole range of thematic classes that can be visible by remotely sensed data, four thematic classes related to forested and nonforested land were identified.

To obtain the data used to train the *k*NN algorithm, at least one polygon was digitized for the spectral documentation of each thematic class supported by ancillary
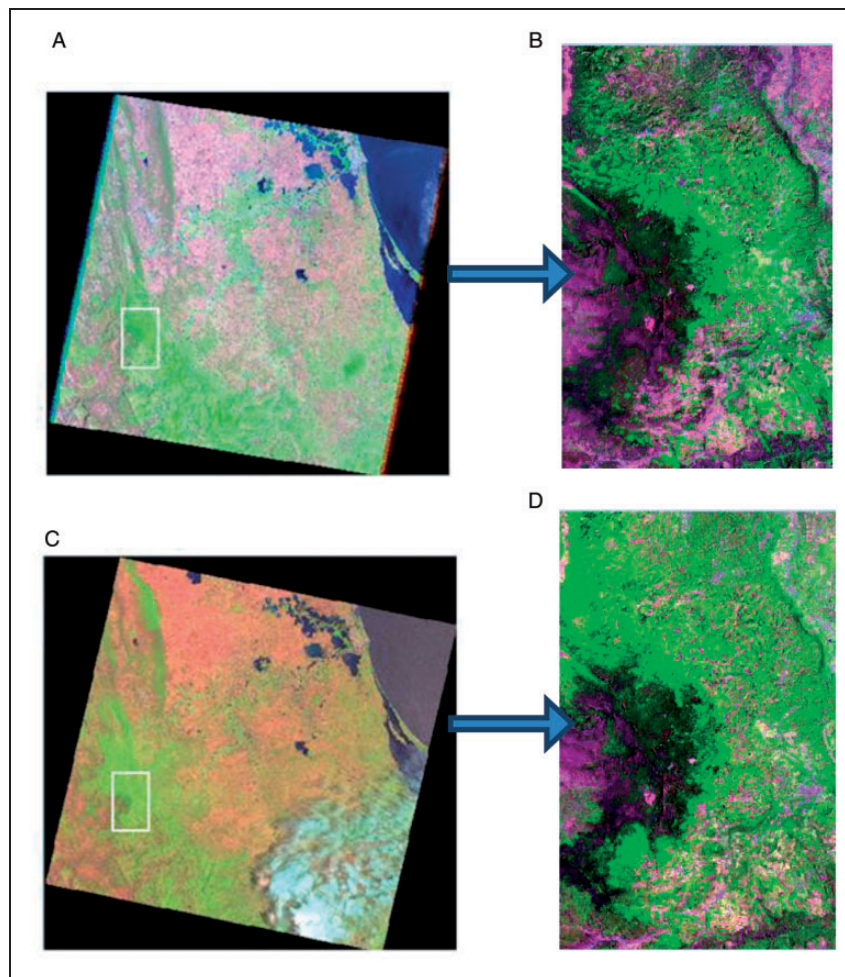
Figure 2. Satellite imagery used. A: Landsat 5 TM image (April 13, 2011). B: False color image (RGB) adjusted to the study area: SWIR1 (B5), NIR (B4), Red (B3). C: Landsat 8 OLI (April 29, 2017). D: False color image (RGB) adjusted to the study area: SWIR1 (B6), NIR (B5), Red (B4).

data (*i.e.*, vegetation and land use map and Cartus et al.'s forest density map) to properly identify each thematic class. For the digitization of polygons used as training fields for the identification of nonforested areas, a threshold of 10 Mg based on the Cartus carbon map was used. Therefore, eight vegetation and land use classes were analyzed. Figure 3 shows the spectral signatures for all classes. Once maps were obtained with eight thematic classes (Figure 4), they were reclassified into two-classes maps: forest and nonforest. For the purpose of determining the areas that have been with no forest over the last five years, the two Boolean maps were overlaid (Figure 5).

To evaluate the map classification reliability, 100 random sample sites were verified via high-spatial-resolution imagery in Google Earth (Figure 6). The validation outcome was analyzed via confusion matrix by determining some reliability parameters, *i.e.*, Kappa, overall, producer, and user accuracies (Chicas et al.,

2016; Lui & Coomes, 2015). The values obtained are as follows: Kappa: 0.735; overall accuracy: 0.95; producer's accuracy: 0.99 for forest and 0.67 for nonforested classes; user's accuracy: 0.96 for forest and 0.89 for nonforested classes. Figure 7 shows the proposed methodological framework to identify eligible areas for carbon capture at the local level by using Landsat imagery.

Estimating the Potential for Above-Ground Carbon Capture

With the intention of estimating the potential for above-ground carbon capture in eligible areas (nonforested), two main data sources were used. First, a land use and land cover map created by the National Forest Inventory of Mexico at 1:50,000 scale was employed (CONAFOR, 2015). This map contains the land use and land cover units/polygons identified by visual
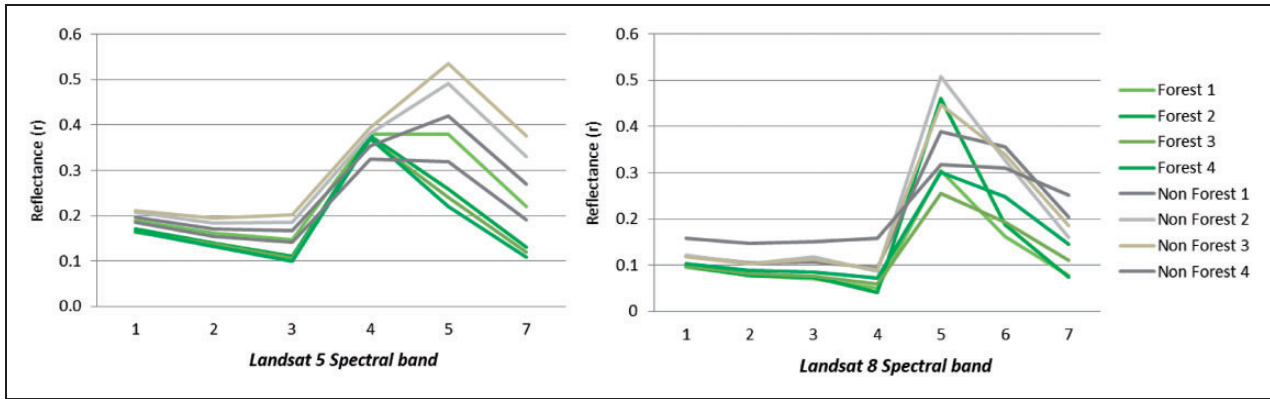
Figure 3. Spectral Signatures Built for Identifying Forest and Non Forest Classes Using Landsat Spectral Data.
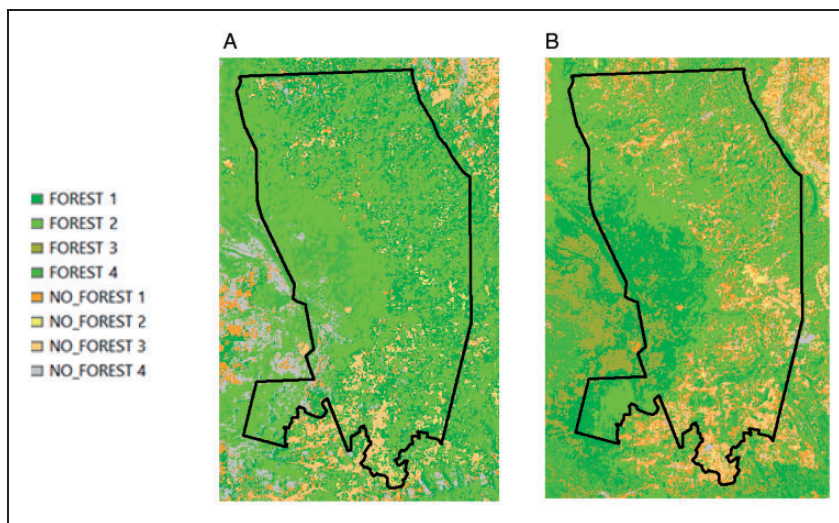
Figure 4. *k*NN Algorithm Applied to the Landsat Spectral Data. A: Landsat 5 TM (2011). B: Landsat 8 OLI (2017).
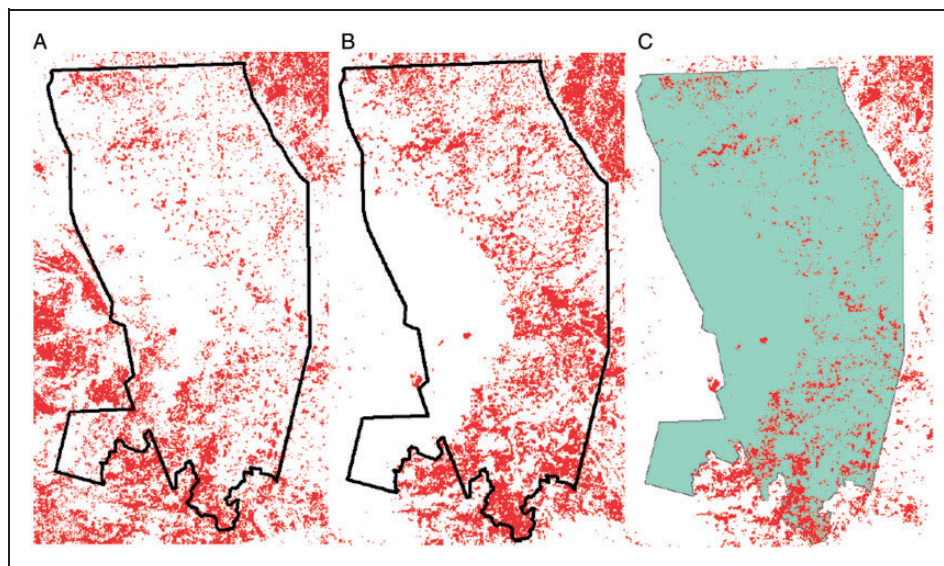
Figure 5. Reclassification Into Two Categories: No Forest (Red) and Forest (White). A: Landsat 5 TM (2011). B: Landsat 8 OLI (2017). C: Potential sites for carbon capture inside the study area by overlaying no forest maps.
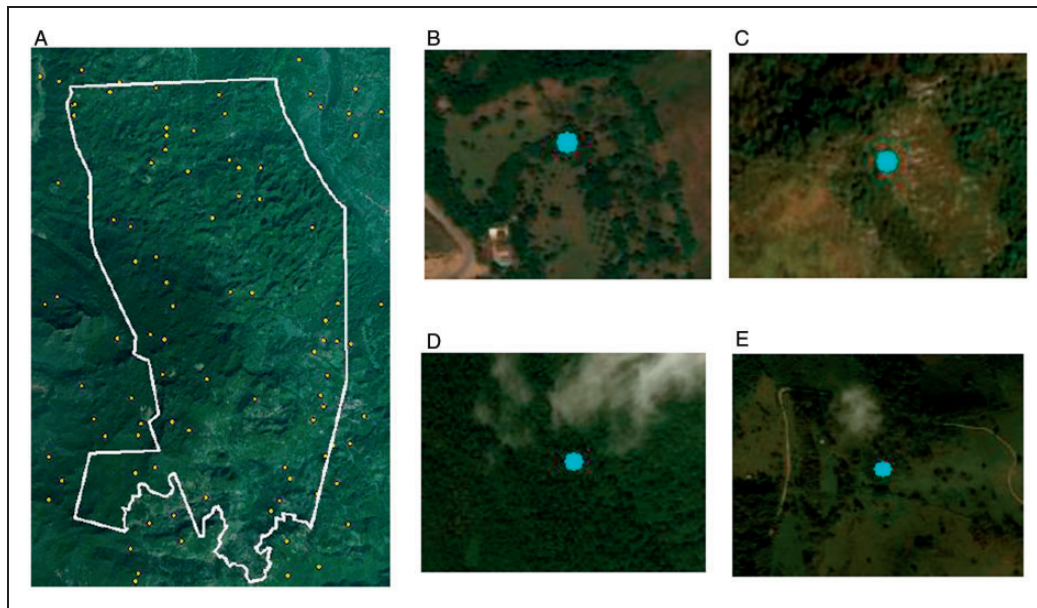
Figure 6. Validation of the *k*NN Classification. A: Spatial distribution of 100 randomly located sample points. B: Case 1: Non forest-forest (considered as an error). C: Case 2: Non forest-non forest (considered as correct). D: Case 3: Forest-forest (considered as correct). E: Case 4: Forest-Non forest (considered as an error).
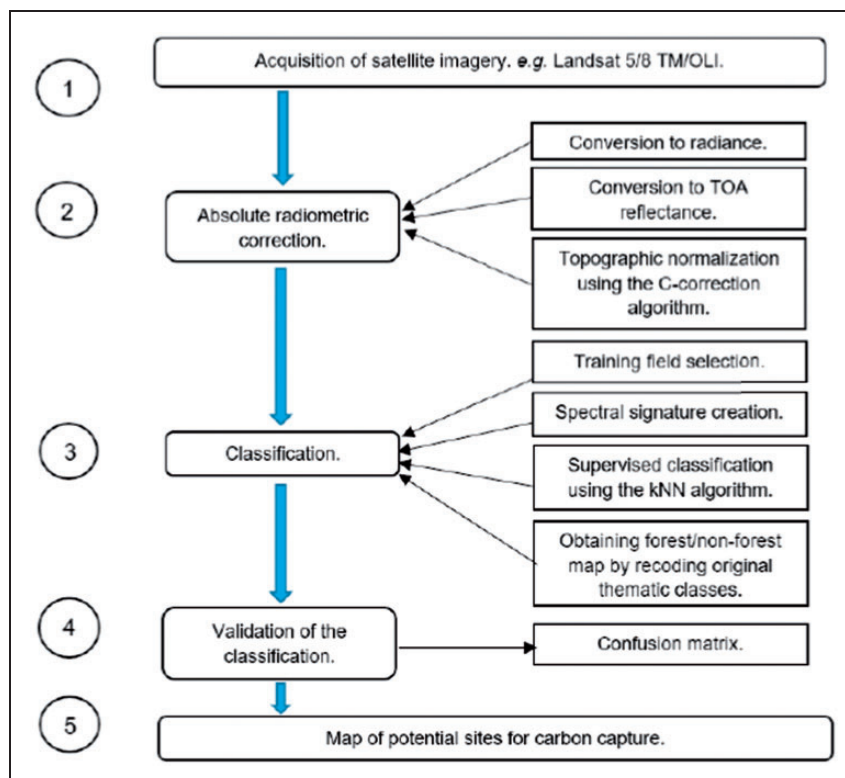
Figure 7. Methodological Flowchart Proposed for the Definition of Eligible Areas for Carbon Capture.

interpretation over high spatial resolution imagery at 4 ha as the minimum mapping unit (Figure 8A). Second, Cartus et al. (2014) created an above-ground carbon map (Mg ha^{-1}) at the national level for Mexico (30 m spatial resolution) (Figure 8B). Two maps were intersected in order to obtain above-ground carbon values (Cartus et al., 2014) for each land use and land cover type (CONAFOR, 2015). Such intersecting was

done by converting carbon values at the pixel level to point and overlaying them against the land cover maps. The purpose of unioning both land use and land cover map to above-ground carbon map was to obtain descriptive statistics for each vegetation type of forested areas, *i.e.*, maximum, minimum and mean above-ground carbon values (Mg C ha^{-1}) (Figure 8C).

The rationale used to determine the potential of aboveground carbon capture was that, from an ecological point of view, tree density in conserved vegetation polygons nearer to eligible areas for carbon capture (nonforested) can be considered as a target to fulfill when capturing forest carbon; thus, their aboveground values can be taken as a reference to be assigned for those neighboring nonforested lands that are eligible for carbon capture. In this way, potential aboveground carbon capture estimation will be influenced by carbon value estimates of adjacent land cover polygons, leading to realistic estimation of potential carbon capture in forests. To make a representative estimate of the potential amount of above-ground carbon that can be captured by a nonforested land, the median between the maximum and average above-ground carbon value of neighboring vegetation was considered, *i.e.*, 75%, with respect to the maximum forest density reported to the polygon in the influence area. Note that the selection of the 75% of forest density as the target density achievable by a new forest stand appears arbitrary. However, we believe that this can be a moderate target forest density between the mean and the maximum forest density reported in the Cartus et al.'s map, in order to obtain realistic estimations.

Therefore, in order to assign those summarized above-ground carbon values, centroids of conserved vegetation polygons were generated to build Thiessen polygons to create their areas of influence (Figure 9A and B). Such polygons are unique because they do not overlap among them, and all locations are nearer to the associated centroid (Alexander et al., 2017). Therefore, the amount of above-ground tree carbon per hectare (Mg C ha^{-1}) is assumed for each eligible area and then extrapolated to the total area of each individual polygon to obtain the potential amount of carbon that an area can reach. This can be supposed by considering that forest restoration would be conducted by using proper species of native vegetation; further, growth rate obtained by restoration activities could be compared with actual growth rate (Chazdon et al., 2016; Hughes et al., 1999).

To ensure the feasibility criterium that land properties are free of legal conflicts, a national spatial database obtained from the National Agrarian Registry (RAN) of 2009 with information related to land property was used. In Mexico, there are three types of land tenure: ejido, comunidad and private property. Further, eligible areas for above-ground carbon capture were intersected with conflict-free land properties based on that previous information. The formula that accounts for the potential above-ground carbon is as follows (equation (1)):

$$CO_2 = \left[\sum_{j=1}^{m} \left[\sum_{i=1}^{n} \left[\frac{\max \delta_i + \bar{\delta}_i}{2} \right] . A_i \right] \right] . [3.66] \qquad (1)$$

where CO_2 is the total amount of capturable carbon dioxide (Mg CO_2); $\max \delta$ and $\bar{\delta}$ are the maximum and mean, respectively, of forest density in above-ground tree carbon (Mg C ha^{-1}) at the pixel level (30 m spatial resolution) estimated by Cartus et al. (2014) and assigned to the area of influence by a Thiessen polygon. Maximum and mean values are considered to account for 75% of maximum forest density when divided by two, and would be assigned to the individual eligible polygon according to Thiessen polygon influence area; i is the i-th individual eligible polygon for above-ground carbon capture in the j-th land property; n is the total number of individual eligible polygons in the j-th land property, m is the total number of land properties, and A_i is the area of each individual eligible polygon (ha). The first term $\left[\sum_{j=1}^{m} \left[\sum_{i=1}^{n} \left[\frac{\max \delta_i + \bar{\delta}_i}{2} \right] . A_i \right] \right]$ represents the total amount of capturable above-ground tree carbon (Mg C), and the multiplicative factor of 3.66 was used to convert it to CO_2 (Mg CO_2) (McPherson et al., 2016). Figure 10 shows the methodological framework proposed to estimate carbon dioxide capture (Mg CO_2) by using geospatial data.

Once the target density for each individual eligible polygon, *i.e.*, 75% of maximum forest density, was calculated, we estimated the amount of years required to achieve such a target density, which, in general terms, it will depend on a series of environmental conditions that either will favor or limit forest growth. Although we agree that there are a number of models to estimate the time required to achieve a certain target forest density, we decided to build a logistic model using data reported in the literature regarding carbon accumulation and time to obtain a coarse estimation for being used as a reference. The general logistic model is as follows:

$$P(t) = \frac{K}{1 + Ae^{-k.t}} \qquad (2)$$

$$A = \frac{K - P_o}{P_o} \qquad (3)$$

where P is the stand density (Mg C ha^{-1}) at time t (years), K is the ecosystem carrying capacity (Mg C ha^{-1}) t, which can be assumed as 72 Mg C ha^{-1} (De
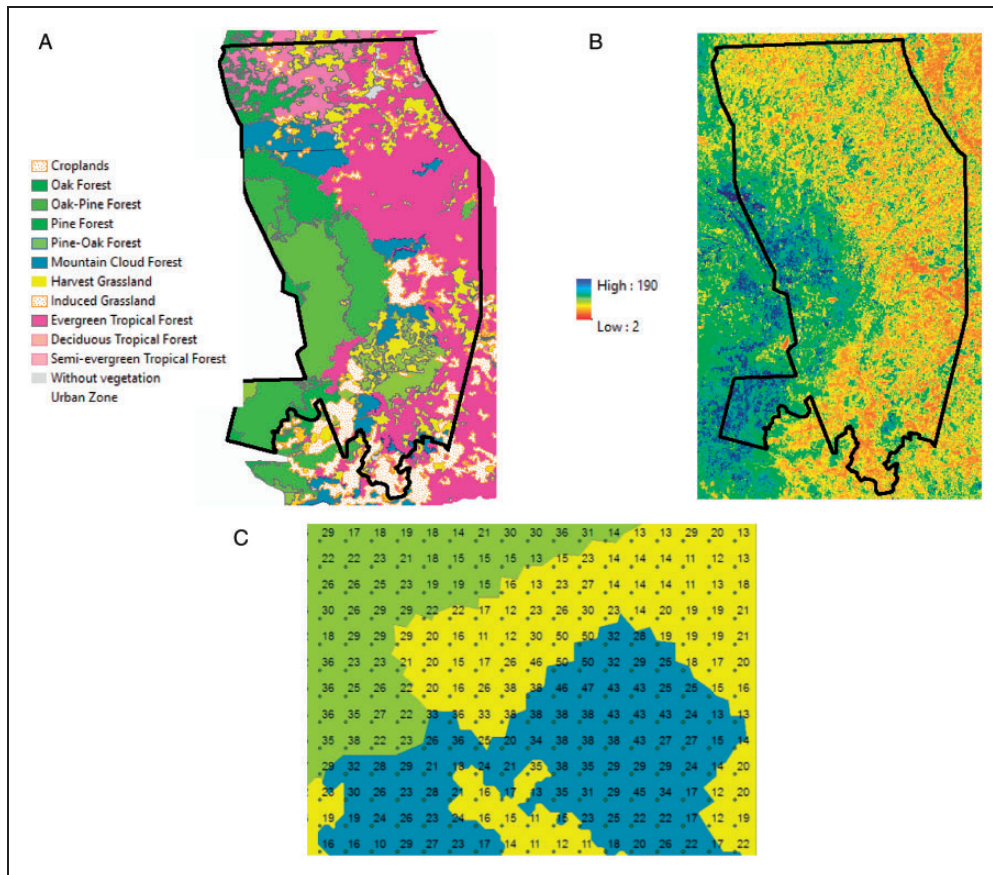
Figure 8. A: Land use and land cover map for the study area created by the National Forest Inventory of Mexico (CONAFOR, 2015). B: Aboveground carbon map in Mg.ha-1 extracted from data provided by Cartus et al. (2014) and clipped for the study area. C: Detailed view of a zoom-in over a specific location inside the study area over Cartus et al.'s data: values represent aboveground carbon estimated at pixel level (30 m spatial resolution).
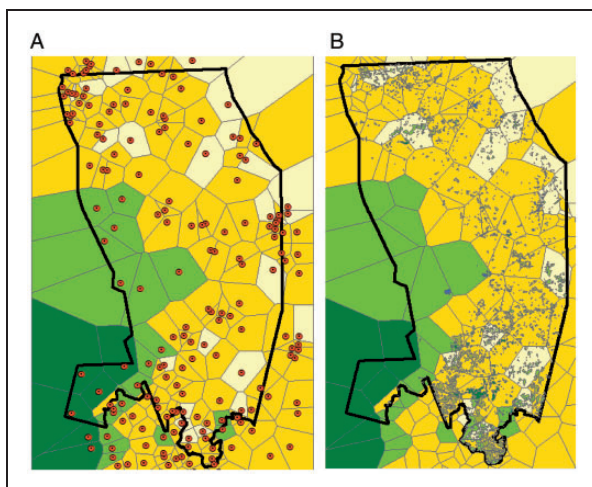
Figure 9. Spatial allocation of target forest density using Thiessen polygons. A: Thiessen polygons obtained by using the centroids of conserved vegetation polygons. B: Intersection with map of potential sites of interest for carbon capture.

Jong et al., 2010), k is a constant of proportionality (dimensionless), and P_o is the initial stand density, equal to 1.6 in Mg C ha^{-1}, for the first year. The model obtained is as follows:

$$T = \frac{\ln\left(\frac{\frac{72}{C}-1}{71}\right)}{\ln 0.9} \qquad (4)$$

where T is the time required to achieve the target forest density (years), and C refers to the target forest density in Mg C ha^{-1}.

Results

Potential Sites for Above-Ground Carbon Capture

After processing the Landsat data taken over the last five years to identify potential sites for carbon capture,
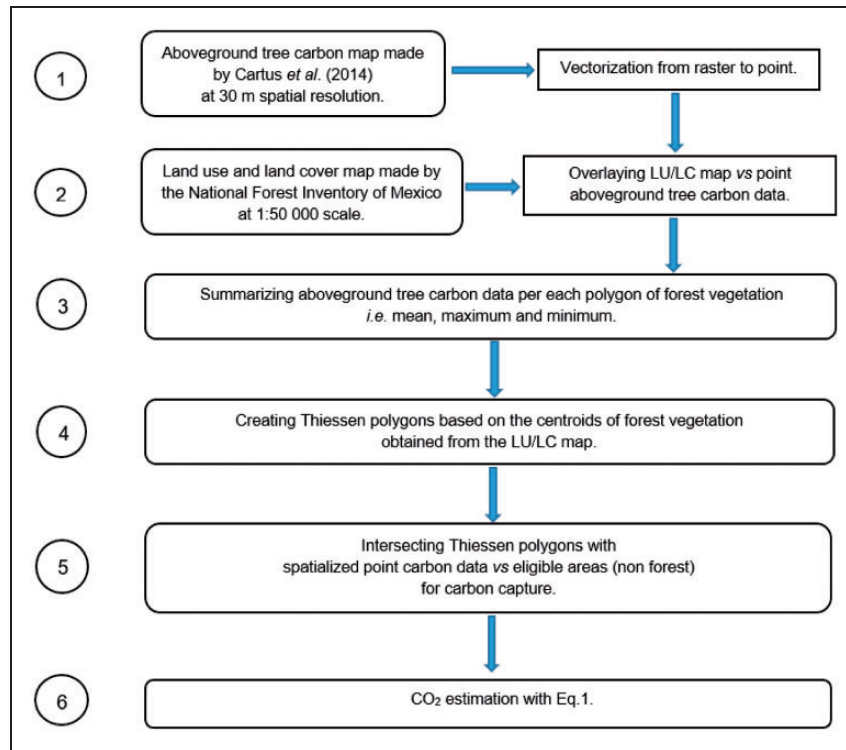
Figure 10. Flowchart of Methodology Proposed to Calculate the Potential Amount of Total Carbon Capture in Eligible Areas.

Table 1. Confusion Matrix to Validate the Map of Potential Sites of Carbon Capture.

Thematic class	Forest	Non forest	Total	User accuracy	Producer accuracy
Forest	87	4	91	0.96	0.99
Non forest	1	8	9	0.89	0.67
Total	88		12	100	
Overall accuracy			0.95		
Kappa index		0.735	**Concordance**	Good	
Standard error			0.116		

the nonforested area estimated for the PRCX was 2,136.1 ha. Such sites revealed a vegetation density lower than 25% from April 2011 to April 2017. The confusion matrix in Table 1 was built on validation data. The map of potential sites shows an overall accuracy of 95% and a kappa of 0.735, meaning that the map has good concordance between the created map against validation data (Chicas et al., 2016).

Eligible sites for carbon capture (sites with no forest over the last five years), according to land tenure class, are as follows: 30 private properties with 957.7 ha, 22 ejidos with 908.47 ha, and three communities with 269.8 ha. However, some of them have land tenure conflicts reported in the official database of land property. Table 2 shows the amount of area of eligible sites for carbon capture with respect to land tenure conflicts; 504.5 ha are free of land tenure conflicts and

have not presented forest cover over the last five years (Table 2).

Potential of Above-Ground Carbon Capture

The potential of capturing above-ground tree carbon and carbon dioxide, under the assumptions of forest restoration (which accounts for density conditions of neighboring vegetation; calculations for the entire study area were obtained by the sum of capturable carbon per each individual eligible site) is presented in Table 3. All polygons that are eligible in the study area can capture in total either 68,807 Mg C or 251,835 Mg CO_2 (Table 3). However, when considering such capture potential for each type of land tenure, the following outcome is obtained: 31,279.7 Mg C for the private-property land tenure (45.4%), 29,512.2 Mg C for the ejido land

Table 2. Legal Situation of Land Tenure in RPCX.

Legal situation of the property	Community (ha)	Ejido (ha)	Private property (ha)	Total (ha)
Regularized land tenure	3.1	501.4	0.0	504.5
Land tenure under litigation	266.7	407.0	0.0	673.8
Information not available	0.0	0.0	957.7	957.7
Total	269.8	908.46	957.7	2,136.0
Percent %	12.6	42.5	44.8	100.0

Table 3. Potential of Aboveground Tree Carbon Capture (Mg C) According to Land Tenure and Legal Criteria.

Legal situation of the property	Community (Mg C)	Ejido (Mg C)	Private property (Mg C)	Total (Mg C)
Regularized land tenure	93.33	16,534.28	0.00	16,627.61
Land tenure under litigation	7,922.16	12,977.97	0.00	20,900.13
Information not available	0.00	0.00	31,279.78	31,279.78
Total	8,015.49	29,512.25	31,279.78	68,807.52

tenure (42.9%), and 8,015.5 Mg C for the community land tenure (11.7%). This capture potential can be achieved considering a long-term scenario (35–40 years) with a biomass growth yield rate of 1.6 Mg C ha^{-1} yr^{-1}, which has been reported in the literature as feasible in average at the national level for coniferous forests (CF) (De Jong et al., 2010). Finally, considering that there is only 504.5 ha free of land tenure conflict, the final amount of capturable above-ground tree carbon is reduced to either 16,627.6 Mg C or 60,857.0 Mg CO_2 distributed in 13 ejidos and two comunities (Table 4).

Discussion

The results obtained in this research lead to a better understanding of the feasibility of a project proposal for above-ground carbon capture to be further promoted and implemented at the local scale. Unlike other studies made for determining the potential amount of carbon capture (Balderas et al., 2014; Torres et al., 2010), this work incorporates the analysis of two basic requirements for the application of the MOS: i) continuity of bare soil conditions since the last five years, and ii) without conflicts of land tenure.

In the PRCX, two studies have been carried out to determine the carbon capture potential. Torres et al. (2010) estimated forest density (above-ground carbon stock) in the Xilitla Reserve by vegetation type using forest inventory techniques. The authors utilized a 1:50,000 scale land use and land cover map previously created by Mesomaya and CONANP (2010) to identify each thematic class within the natural protected area (33,949.4 ha). Above-ground carbon potential was estimated from current annual increments, depending on the species. The authors also found that annual above-ground potential capture for the entire study area is

equal to 179,682 Mg CO_2 yr^{-1}. The authors, however, did not consider above-ground carbon capture as a gain from reforestation, forestation, or forest restoration but from current annual increments of already forested land; the authors also did not separate conflict-free land tenure. The second, developed by Balderas et al. (2014), was reported to determine forest carbon capture in the study area at the regional level. In this research work, unlike in Torres et al.'s work, the authors considered an area of 6,820 ha of nonforested land (agricultural and pasture use) as suitable to capture forest carbon; the estimates of forest carbon capture were calculated using standard values taken from IPCC, *i.e.*, for Tier 1 was 25,727 Mg CO_2 yr^{-1}, for Tier 2 was 5,989 Mg CO_2 yr^{-1}, for Tier 3 was 13,895 Mg CO_2 yr^{-1}. Such tiers represent an assumed reduction in the uncertainty of estimates. Such an approach is at the regional level, lacks social criteria for eligibility, and is not suitable for our objective.

At the global level, other recent modeling experiences on potential land for forest restoration have been reported. Brancalion et al. (2019) mapped the potential land for forest restoration by estimating a compound index, *i.e.*, the restoration opportunity score (ROS). To identify target areas, the authors first used a threshold of 90% tree canopy cover over a global land cover map, and then masked out urban areas, water bodies, and wetlands. Subsequently, they scored target areas by considering the following criteria: 1) restoration benefits, including biodiversity conservation, climate change mitigation and adaptation, and water security and 2) restoration feasibility, that is land opportunity costs, landscape variation in forest restoration success and persistence changes of restored forests. However, the authors warned that implementation of forest restoration might additionally depend on other

Table 4. Potential Carbon Capture for Ejidos and Comunities That Meet Both Eligibility and Feasibility Criteria in the RPCX.

Land tenure	Name of either Ejido or community	Area of eligible site for carbon capture (ha)	Capture potential (Mg C ha-1)	Capture potential of aboveground tree carbon (Mg C)	Years	Capture potential of carbon dioxide (Mg CO$_2$)
Ejido	Soledad de Zaragoza	162.57	32.9	5,352.58	38.8	19,590.44
	Miramar	124.31	30.8	3,829.16	37.7	14,014.73
	Ollita del pino	83.96	32.9	2,759.74	38.8	10,100.65
	Coronel Castillo	66.05	37.5	2,475.57	41.2	9,060.59
	Apetzco	23.84	30.4	725.19	37.5	2,654.20
	Xilitlilla	14.51	30.7	445.82	37.7	1,631.70
	Aguayo	12.92	44.6	575.61	45.1	2,106.73
	Amayo de Zaragoza	9	25.5	229.5	34.8	839.97
	San Antonio Xalcuayo	2.68	33.9	90.73	39.3	332.07
	Ahuacatlán	0.87	34	29.57	39.4	108.23
	Xuchiayo	0.57	30.4	17.34	37.5	63.46
	San José de Hoyja	0.12	21.4	2.57	32.3	9.4
	Bagazo	0.03	30	0.9	37.3	3.29
Community	Sazn Antonio Xalcuayo	1.95	26.4	51.5	35.3	188.49
	Cañón de Tlamaya	1.15	36.4	41.83	40.7	153.1
	Total	504.53	33	16,627.61	38.8	60,857.05

socio-environmental factors, including land tenure security, local disturbance factors, or legal regulations, while Bastin et al. (2019) mapped the potential tree cover at the global level by using a random forest algorithm fueled with data to depict the entire range of both environmental (climate, soil and topography) and forest density conditions. The pixels in this map represent potential tree forest density (% forest cover) that the ecosystem would be able to thrive according to a set of environmental conditions and with minimal human intervention. They also argue that, because they did not have data on land tenure at the global level, it is still difficult to estimate how much land is really available for forest restoration. Therefore, to ensure the feasibility of a forest carbon capture project overtime, there should be clarity in regard to who is the land owner (public or private), *i.e.*, land requires to be conflict free of land tenure.

In the 3rd National Communication of the GHG inventory, Mexico reported a mean value of aboveground tree carbon of 52 Mg C ha^{-1} for tropical rainforest, including evergreen and seasonal rainforest; for the case of lands classified as nonforested, carbon values varied from 6 to 19 Mg C ha^{-1} (De Jong et al., 2010). In our work, the same vegetation type exhibited forest density values from 18 Mg C ha^{-1} to 91 Mg C ha^{-1} (average of 54.5 Mg C ha^{-1}), while the sites considered as noforest presented a mean vegetation density value of 14.67 Mg C ha^{-1}. Therefore, these mean values of above-ground tree carbon are similar to those reported at the national level for Mexico.

Several growth rates in other countries are reported at different ecological conditions. In Peru's mountain cloud forests, for example, growth rates can vary from 9 Mg C ha^{-1} yr^{-1} at 3,000 m.a.s.l. until 21 Mg C ha^{-1} yr^{-1} at 1,000 m.a.s.l. (Malhi et al., 2017). In Ecuador's cloud forests, growth rates can range from 4 Mg C ha^{-1} yr^{-1} at 2,250 m.a.s.l until 10 Mg C ha^{-1} yr^{-1} at 1,000 m.a.s.l. during the first five to seven years after natural forest regeneration; such growth rates decrease to 1–2 Mg C ha^{-1} yr^{-1} after 12 to 15 years (Spracklen & Righelato, 2016). Although forest growth rate depends on a variety of factors (*e.g.*, ecological interactions, species-specific, biogeographical conditions), in the tropics, elevation is a major factor strongly linked to mean annual temperature, which directly influences forest growth either favouring or limiting it.

In Mexico, there are several examples of estimating forest growth rate in forested ecosystems similar to our study area. In tropical forests located in the region of Los Tuxtlas en Veracruz, Hughes et al. (1999) found that biomass accumulation on soil varied from 2.3 to 18.3 Mg C ha^{-1} yr^{-1}, which is inversely correlated to the time that soil has been used for crop production. In liquidambar forests growing in steep slopes with altered vegetation conditions in the northern mountains of Oaxaca, the mean growth rate was of 2.5–3 Mg C ha^{-1} yr^{-1} during the first 40 years, while in sites with secondary vegetation, forest growth rate varied from 2.5 to 5 Mg C ha^{-1} yr^{-1} (Etchevers et al., 2001). Aryal et al. (2014) found that the biomass accumulation rate in Calakmul's biosphere is of 3.0 Mg C ha^{-1} yr^{-1} for four- to 10-year-old forests and 1.6 Mg C ha^{-1} yr^{-1} for 35-year-old forests.

In all cases, the forest growth rate will depend on the current successional stage after abandonment (Aryal et

al., 2014; Etchevers et al., 2001; Figueroa-Navarro et al., 2005; Hughes et al., 1999; Malhi et al., 2017). Although growth can be modeled with sigmoid/logistic curves to better represent forest sucession stages, in this research, we assumed a growth rate for a humid tropical forest of $1.6\,\text{Mg C ha}^{-1}\text{yr}^{-1}$ to estimate the potential of above-ground tree carbon growth. Mexico used this rate in its 3rd National Communication of GHG emissions presented at the UNFCCC-COP 12; this was the first inventory with the most information derived from national sources, Tier 2 (De Jong et al., 2010). Using this growth rate allowed us to calculate the time required by a forest to reach the top forest density condition as a mature vegetation and estimate planning over time with realistic data.

In order to define the above-ground tree carbon potential that an eligible site could gain, a threshold of 75%, with respect to the maximum forest density recorded in the Cartus et al. (2014) map, was assigned. To do this, neighboring vegetation type was also considered in threshold allocation by using Thiessen polygons to delineate their influence areas. This approach was carried out by combining remotely sensed above-ground carbon data estimates with geospatial data, *i.e.*, vegetation map at 1:50,000 scale to predict the most probable density in a matured forest. The Thiessen polygon approach was used in the forest sector to analyze variables strongly linked to spatial features of a forest such as stand age, land tenure, and physiognomic characteristics of trees, *i.e.*, tree crown height (Argamosa et al., 2016; Butler et al., 2014; Nelson et al., 2004).

In the study area, each eligible site presents varying growth and environmental conditions. This approach gives a customized estimate of above-ground tree carbon for each eligible site. For example, a forest stand could be within the influence of a seasonally dry tropical forest with a forest carbon capture potential of $38\,\text{Mg C ha}^{-1}$ or within an influence area of an evergreen rainforest with a forest carbon capture potential of $72\,\text{Mg C ha}^{-1}$. According to the literature, the first example could reach a mature level during a 30- to 40-year period, while the second will require a 60- to 65-year period (Etchevers et al., 2001). This leads us to reveal that such forest restoration will be achieved in very different time lapses (Aryal et al., 2014; Etchevers et al., 2001).

In tropical forests, the time required for carbon stocks to be fully recovered is approximately between 73 and 85 years (Hughes et al., 1999; Martin et al., 2013; Spracklen & Righelato, 2016) or until 125 years old (Aryal et al., 2014). These types of ecosystems feature other carbon reservoirs, including understory, dead wood, and leaf litter under natural regeneration conditions. This is mainly because forest growth rates are non-linear and depend on vegetation type (Sherman et al.,

2012). During the forest restoration process, commonly occurring changes are associated with the gain/loss of individual trees of new species.

As time progresses, recruitment of new species decreases and mortality of trees increases. This process is accompanied by a change of dominance from softwood to hardwood tree species, thus explaining the extensive time a forest requires to recover until its previous stage before perturbation (Aryal et al., 2014). On this basis, in the present work, we observed that the time period for reaching the maximum forest density would be at least greater than 20 years. Thus, we tried to model the time length using a logistic model constructed in a deterministic way, by considering the limits of forest carbon density and the time required for it, after literature review. The required time obtained for forests to grow to meet a target density was over 35 to 40 years; however, in real-world conditions, it depends on a number of factors, *e.g.*, species growth rate (fast-growth species, precipitation regime, soil depth, soil nutrients available, among others). Therefore, this estimate is only to obtain a general idea of the required length of time for a forest to reach its desired density.

To know how long an eligible area takes to reach its maximum potential for carbon capture, it is mandatory to define particular environmental and ecological growth conditions and further apply a methodology for modeling forest growth as a whole, from different points of view, *e.g.*, empirical (allometric equations) or physiological (biophysical models) (Vanclay, 1994). Researchers have developed a number of tools on this subject that can be used for estimating forest growth, considering selected species and the productive capacity of soil. Some models that allow estimating such approximations include the forest vegetation simulator (FVS) (Crookston & Dixon, 2005), the carbon budget model of the Canadian forest sector (CBM-CFS3) (Kurz et al., 2009), and the tropical rain forest stand table projection (Vanclay, 1995).

This research assumed that nonforested places nearer to natural vegetation should exhibit the same vegetation type because they will probably share the same environmental conditions. However, other approaches could be explored to assign vegetation type not only to the nearer one but to the most similar, according to environmental conditions in the feature space, *i.e.*, multivariate space. It would be interesting to compare the differences between the two approaches, *i.e.*, geographical versus feature space. Probably, using geographical space to assign the most suitable vegetation type would derive a more homogeneous landscape than that obtained by considering an environmental multivariate feature space. Evaluating these two alternatives in terms of biodiversity conservation, for example, may be challenging because

they could reveal possibilities in the future landscape configuration.

One important point to highlight in this research was the availability of a high spatial resolution carbon map for the whole country (Cartus et al., 2014). This seamless data set was used to estimate forest density in terms of above-ground tree carbon (Mg C) inside vegetation polygons depicted at the 1:50 000 scale, empowering the most detailed land use land cover map available to spatially describe forest carbon at the local level. Cartus et al.'s map of forest density was multidated because it was created with multiple data sources, i.e., forest inventory data gathered by sampling from 2004–2007, Landsat data collected during 2004–2007, and the land use land cover map series IV made by photo-interpretating Landsat and SPOT imagery were taken from 2007 and 2008.

Even though it is challenging to have an actual map of forest density at the national level on a year-by-year basis, the approximations carried out in this work of forest carbon using Cartus et al.'s data currently represent the most updated estimates that can be achieved with official data sets at high spatial resolution. Therefore, these comprehensive forest carbon estimates worked well because they were done by calculating descriptive statistics, i.e., maximum and mean above-ground tree carbon value, using all pixels from Cartus et al.'s data for each land cover polygon at 1:50 000 scale to know the potential capacity of forest carbon capture of eligible sites using neighboring vegetation information.

Further efforts of forest density data creation will make it easier to design these types of projects. Recently, it was announced that the accessibility of a globally available seamless data set of forest/nonforest at 50 m spatial resolution that was built with active remote sensing data (TanDEM-X interferometric data) (Martone et al., 2018). This kind of information will be useful in a number of ways. For example, as a validation data source for the current nonforest map creation or if forest carbon values are available in additional versions of this data set, it can be used as the Cartus et al.'s. map for above-ground carbon data source at the global level.

The area of nonforested land estimated in this work by using remote-sensing techniques was of 2,136 ha, with an estimate of above-ground tree carbon capture of 68,807 Mg C, equivalent to 251,835 Mg CO_2. However, estimating the potential of forest carbon capture is more complex in tropical regions due to a diversity of ecological, climatological, soil, topographical, and biogeographical conditions (Malhi et al., 2017).

On the other hand, although these outcomes appear promising, a special issue was detected when examining omission and comission error rates between classes in the 2017 map. The producer's accuracy obtained for nonforested was 0.67. This can lead to important errors in areal estimation. Hall (1994) stated that, when classification error rates are about 20%, areal estimation errors may be yielded as 10%. Thus, in this research, if errors are approximately 33%, areal estimation errors could be between 15% and 20%. This suggests that further studies must be oriented to use more detailed spatial resolution remotely sensed data sources (i.e., < 10 m spatial resolution) to fulfill accuracy requirements to map nonforested land in a finer way.

Forest carbon stocks usually include above- and below-ground carbon. However, the MOS was initially designed to account for only aboveground carbon, without detriment to consider soil carbon in quantifications; therefore, taking soil carbon into account may be optional when setting up forest carbon capture projects (Ministry of Economy, 2015). Still, soil accumulates a significant amount of carbon that should be considered in carbon capture projects. Then, incorporating soil carbon estimates into the methodology as further research may increase certainty on how carbon is being fixed after establishing a forest carbon capture project. To date, only one study estimates soil carbon at 250 m spatial resolution for the conterminous United States and Mexico (Guevara et al., 2020). This data set may be used as a reference to calculate soil carbon gains or additionality.

Implications for Conservation

The methodology presented here may be used as a reference for those interested in promoting forest development by identifying the sites that may be eligible in the implementation of a carbon sequestration project. Further effort will be required to downscale the outcomes of this approach, by using higher spatial resolution remotely sensed data sources, i.e., < 10 m spatial resolution. The project developer must work between the forest owners and the purchaser of the ex ante carbon credits to compensate, partially or totally, the carbon footprint generated in its production, distribution, or operation processes. In the NMX-AA-173-SCFI-2015 standard, the mechanisms to be followed for the design of these type of projects are published. Reforestation, forestation, and forest restoration as the result of the implementation of these projects may also strengthen biodiversity conservation by increasing forest cover with local species and improve connectivity in highly fragmented landscapes. Thiessen polygons can also be used for allocating what species to plant or foster to grow in each individual eligible polygon. The main goal of our approach is to create a methodology for finding those places that can be restored to their initial stage before land conversion and degradation. This approach is applicable for countries interested in

identifying potential areas for forest carbon capture and encouraging carbon's credit economic growth for empowering rural people in cultivating and protecting forests.

ORCID iD

Carlos Arturo Aguirre-Salado (iD) https://orcid.org/0000-0003-3422-7193

References

Alexander, C., Korstjens, A. H., & Hill, R. A. (2017). Structural attributes of individual trees for identifying homogeneous patches in a tropical rainforest. *International Journal of Applied Earth Observation and Geoinformation*, 55, 68–72. http://dx.doi.org/10.1016/j.jag.2016.11.004

Anaya, J. A., Chuvieco, E., & Palacios-Orueta, A. (2009). Aboveground biomass assessment in Colombia: A remote sensing approach. *Forest Ecology and Management*, 257(4), 1237–1246. https://doi.org/10.1016/j.foreco.2008.11.016

Argamosa, R. J. L., Paringit, E. C., Quinton, K. R., Tandoc, F. A. M., Faelga, R. A. G., Ibañez, C. A. G., Posilero, M. A. V., & Zaragosa, G. P. (2016). Fully automated GIS-based individual tree crown delineation based on curvature values from a lidar derived canopy height model in a coniferous plantation. *International Archives of the Photogrammetry, Remote Sensing & Spatial Information Sciences*, 41. https://doi.org/10.5194/isprsarchives-XLI-B8-563-2016

Aryal, D. R., De Jong, B. H., Ochoa-Gaona, S., Esparza-Olguín, L., & Mendoza-Vega, J. (2014). Carbon stocks and changes in tropical secondary forests of Southern Mexico. *Agriculture, Ecosystems & Environment*, 195, 220–230. https://doi.org/10.1016/j.agee.2014.06.005

Balderas, A., Ross, D., Hernández, J. C., & de Alba, H. (2014). *Estimación y valoración de los acervos y potencial de captura de carbono en cuatro áreas protegidas de la Sierra Madre Oriental* [Estimation and valuation of the stocks and potential of carbon sequestration in four protected areas of the Eastern Sierra Madre]. Comisión nacional de áreas naturales protegidas (CONANP) y deutsche gesellschaft für internationale zusammenarbeit (GIZ) GmbH. https://bit.ly/3dAJiTV

Bastin, J. F., Finegold, Y., García, C., Mollicone, D., Rezende, M., Routh, D., Zohner, C. M., & Crowther, T. W. (2019). The global tree restoration potential. *Science (New York, N.Y.)*, 365(6448), 76–79. https://doi.org/10.1126/science.aax0848

Brancalion, P. H. S., Niamir, A., Broadbent, E., Crouzeilles, R., Barros, F. S. M., Almeyda Zambrano, A. M., Baccini, A., Aronson, J., Goetz, S., Reid, J. L., Strassburg, B. B. N., Wilson, S., & Chazdon, R. L. (2019). Global restoration opportunities in tropical rainforest landscapes. *Science Advances*, 5(7), eaav3223. https://doi.org/10.1126/sciadv.aav3223

Breidenbach, J., Næsset, E., & Gobakken, T. (2012). Improving k-nearest neighbor predictions in Forest inventories by combining high and low density airborne laser scanning data. *Remote Sensing of Environment*, 117, 358–365. https://doi.org/10.1016/j.rse.2011.10.010

Butler, B. J., Hewes, J. H., Liknes, G. C., Nelson, M. D., & Snyder, S. A. (2014). A comparison of techniques for generating Forest ownership spatial products. *Applied Geography*, 46, 21–34. http://dx.doi.org/10.1016/j.apgeog.2013.09.020

Cartus, O., Kellndorfer, J., Walker, W., Franco, C., Bishop, J., Santos, L., & Fuentes, J. M. (2014). A national, detailed map of Forest aboveground carbon stocks in Mexico. *Remote Sensing*, 6(6), 5559–5588. https://doi.org/10.3390/rs6065559

Chazdon, R. L., Broadbent, E. N., Rozendaal, D. M. A., Bongers, F., Zambrano, A. M. A., Aide, T. M., Balvanera, P., Becknell, J. M., Boukili, V., Brancalion, P. H. S., Craven, D., Almeida-Cortez, J. S., Cabral, G. A. L., de Jong, B., Denslow, J. S., Dent, D. H., DeWalt, S. J., Dupuy, J. M., Durán, S. M., ... Poorter, L. (2016). Carbon sequestration potential of second-growth Forest regeneration in the Latin American tropics. *Science Advances*, 2(5), 1–10. https://doi.org/10.1126/sciadv.1501639

Chicas, S. D., Omine, K., & Saqui, P. (2016). CLASlite algorithms and social surveys to asses and identify deforestation and forest degradation in Toledo's protected areas and forest ecosystems. *Applied Geography*, 75, 144–155. https://doi.org/10.1016/j.apgeog.2016.08.012

Chubey, M. S., Franklin, S. E., & Wulder, M. A. (2006). Object-based analysis of ikonos-2 imagery for extraction of forest inventory parameters. *Photogrammetric Engineering & Remote Sensing*, 72(4), 383–394.

Cohen, W., Healey, S., Yang, Z., Stehman, S., Brewer, C., Brooks, E., Gorelick, N., Huang, C., Hughes, M. J., Kennedy, R. E., Loveland, T. R., Moisen, G. G., Schroeder, T. A., Vogelmann, J. E., Woodcock, C. E., Yang, L., & Zhu, Z. (2017). How similar are Forest

disturbance maps derived from different landsat time series algorithms? *Forests*, *8*(4), 98. https://doi.org/10.3390/f8040098

CONAFOR. (2015). *Cartografía de los recursos forestales 1:50 000 municipio de xilitla y aquismón. In: Inventario estatal forestal y de suelos* [Mapping of forest resources 1:50 000 municipality of xilitla and aquismón. In: State forest and soil inventory]. SEMARNAT-CONAFOR.

Crookston, N. L., & Dixon, G. E. (2005). The Forest vegetation simulator: A review of its structure, content, and applications. *Computers and Electronics in Agriculture*, *49*(1), 60–80. https://doi.org/10.1016/j.compag.2005.02.003

De Jong, B., Anaya, C., Masera, O., Olguín, M., Paz, F., Etchevers, J., Martínez, R. D., Guerrero, G., & Balbontín, C. (2010). Greenhouse gas emissions between 1993 and 2002 from land-use change and forestry in Mexico. *Forest Ecology and Management*, *260*(10), 1689–1701. https://doi.org/10.1016/j.foreco.2010.08.011

Edwards, A. J. (1998). *Lesson 3: Radiometric correction of satellite images: When and why radiometric correction is necessary*. http://www.ncl.ac.uk/tcmweb/bilko/module7/lesson3.pdf

Etchevers, J., Acosta, M., Monreal, C., Quednow, K., & Jiménez, L. (2001). Los stocks de carbono en diferentes compartimientos de la parte aérea y subterránea en sistemas forestales y agrícolas de ladera en méxico [Carbon stocks in different compartments of the aerial and underground part in forestry and agricultural hillside systems in Mexico]. In *Memorias Del Simposio Internacional Medición y Monitoreo de la Captura de Carbono en Ecosistemas Forestales* (Vol. 18).

Figueroa-Navarro, C., Etchevers-Barra, J. D., Velázquez-Martínez, A., & Acosta-Mireles, M. (2005). Concentración de carbono en diferentes tipos de vegetación de la sierra norte de Oaxaca [Carbon concentration in different types of vegetation of the northern sierra of Oaxaca]. *Terra Latinoamericana*, *23*(1), 57–64.

Freeman, E. A., Moisen, G. G., Coulston, J. W., & Wilson, B. T. (2016). Random forests and stochastic gradient boosting for predicting tree canopy cover: Comparing tuning processes and model performance. *Canadian Journal of Forest Research*, *46*(3), 323–339.

Gallaun, H., Zanchi, G., Nabuurs, G. J., Hengeveld, G., Schardt, M., & Verkerk, P. J. (2010). EU-wide maps of growing stock and above-ground biomass in forests based on remote sensing and field measurements. *Forest Ecology and Management*, *260*(3), 252–261.

Gómez, C., White, J. C., & Wulder, M. A. (2011). Characterizing the state and processes of change in a dynamic Forest environment using hierarchical spatio-temporal segmentation. *Remote Sensing of Environment*, *115*(7), 1665–1679. https://doi.org/10.1016/j.rse.2011.02.025

Gómez, C., Wulder, M. A., White, J. C., Montes, F., & Delgado, J. A. (2012). Characterizing 25 years of change in the area, distribution, and carbon stock of Mediterranean pines in Central Spain. *International Journal of Remote Sensing*, *33*(17), 5546–5573. https://doi.org/10.1080/01431161.2012.663115

Gómez, C., White, J. C., Wulder, M. A., & Alejandro, P. (2014). Historical Forest biomass dynamics modelled with landsat spectral trajectories. *ISPRS Journal of Photogrammetry and Remote Sensing*, *93*, 14–28. https://doi.org/10.1016/j.isprsjprs.2014.03.008

Guevara, M., Arroyo, C., Brunsell, N., Cruz, C. O., Domke, G., Equihua, J., Etchevers, J., Hayes, D., Hengl, T., Ibelles, A., Johnson, K., Jong, B., Libohova, Z., Llamas, R., Nave, L., Ornelas, J. L., Paz, F., Ressl, R., Schwartz, A., … Vargas, R. (2020). Soil organic carbon across Mexico and the conterminous United States (1991–2010). *Global Biogeochemical Cycles*, *34*(3), e2019GB006219. https://doi.org/10.1029/2019GB006219

Hall, F. G. (1994). Potential use of military and space remote sensing technologies to address ecological information needs. In A. Sample (Ed.), *Remote sensing in ecosystem management* (p. 310). Island Press.

Hughes, R. F., Kauffman, J. B., & Jaramillo, V. J. (1999). Biomass, carbon, and nutrient dynamics of secondary forests in a humid tropical region of Mexico. *Ecology*, *80*(6), 1892–1907. http://www.jstor.org/stable/176667

INECC/SEMARNAT. (2015). *Primer Informe Bienal de Actualización ante la Convención Marco de las Naciones Unidas sobre el cambio Climático* [First biennial update report to the united nations framework convention on climate change]. Instituto Nacional de Ecología y Cambio Climático y Secretaria de Medio Ambiente y Recursos Naturales.

Kim, D., Sexton, J., Noojipady, P., Huang, C., Anand, A., Channan, S., Feng, M., & Townshend, J. (2014). Global, landsat-based Forest-cover change from 1990 to 2000. *Remote Sensing of Environment*, *155*, 178–193. https://doi.org/10.1016/j.rse.2014.08.017

Kurz, W. A., Dymond, C. C., White, T. M., Stinson, G., Shaw, C. H., Rampley, G. J., Smyth, C., Simpson, B. N., Neilson, E. T., Trofymow, J. A., Apps, M. J., & Metsaranta, J. (2009). CBM-CFS3: A model of carbon-dynamics in forestry and land-use change implementing IPCC standards. *Ecological Modelling*, *220*(4), 480–504. https://doi.org/10.1016/j.ecolmodel.2008.10.018

Lui, G. V., & Coomes, D. A. (2015). A comparison of novel optical remote sensing-based technologies for Forest-cover/change monitoring. *Remote Sensing*, *7*(3), 2781–2807. https://doi.org/10.3390/rs70302781

Malhi, Y., Girardin, C. A., Goldsmith, G. R., Doughty, C. E., Salinas, N., Metcalfe, D. B., Huasco, W. H., Silva-Espejo, J. E., Aguilla-Pasquell, J., Amezquita, F. F., Aragão, L. E., Guerrieri, R., Yoko, F. I., Bahar, N. H. A., Farfan-Rios, W., Phillips, O. L., Meir, P., & Silman, M. (2017). The variation of productivity and its allocation along a tropical elevation gradient: A whole carbon budget perspective. *The New Phytologist*, *214*(3), 1019–1032. https://doi.org/10.1111/nph.14189

Martin, P. A., Newton, A. C., & Bullock, J. M. (2013). Carbon pools recover more quickly than plant biodiversity in tropical secondary forests. *Proceedings of the Royal Society B: Biological Sciences*, *280*(1773), 20132236. https://doi.org/10.1098/rspb.2013.2236

Martone, M., Rizzoli, P., Wecklich, C., González, C., Bueso-Bello, J. L., Valdo, P., Schulze, D., Zink, M., Krieger, G., & Moreira, A. (2018). The global forest/non-forest map from TanDEM-X interferometric SAR data. *Remote Sensing of Environment*, *205*, 352–373. https://doi.org/10.1016/j.rse.2017.12.002

McPherson, E. G., van Doorn, N. S., & Peper, P. J. (2016). Urban tree database and allometric equations. *General Technical Report*. *PSW-GTR-253*. US Department of Agriculture, Forest Service, Pacific Southwest Research Station.

McRoberts, R. E. (2008). Using satellite imagery and k-nearest neighbors technique as a bridge between strategic and management Forest inventories. *Remote Sensing of Environment*, *112*(5), 2212–2221. https://doi.org/10.1016/j.rse.2007.07.025

Mesomaya, A. C., & CONANP. (2010). *Iniciativa de méxico Para la protección del clima en el corredor ecológico sierra madre Oriental y en las lagunas costeras Laguna madre y marismas nacionales (Cambio climático en ANP's)* [Mexico initiative for climate protection in the Sierra Madre Oriental ecological corridor and in the coastal lagoons Laguna Madre and national marshes (Climate change in ANP's)]. Informe final. ASERCA-Comisión Nacional de Áreas Naturales Protegidas CONANP. https://bit.ly/3cABYIh

Ministry of Economy. (2015, June). *15 Mexican Standard NMX-AA-173-SCFI-2015, for the registration of carbon forestry projects and the certification of the increase in the carbon stock*. http://www.economia-nmx.gob.mx/normas/nmx/2010/nmx-aa-173-scfi-2015.pdf

Neigh, C. S. R., Masek, J. G., Bourget, P., Rishmawi, K., Zhao, F., Huang, C., Cook, B. D., & Nelson, R. F. (2016). Regional rates of young US Forest growth estimated from annual landsat disturbance history and IKONOS stereo imagery. *Remote Sensing of Environment*, *173*, 282–293. https://doi.org/10.1016/j.rse.2015.09.007

Nelson, T., Boots, B., Wulder, M., & Feick, R. (2004). Predicting Forest age classes from high spatial resolution remotely sensed imagery using voronoi polygon aggregation. *GeoInformatica*, *8*(2), 143–155. https://doi.org/10.1023/B:GEIN.0000017745.92969.31

Nelson, R., Margolis, H., Montesano, P., Sun, G., Cook, B., Corp, L., Andersen, H.-E., deJong, B., Pellat, F. P., Fickel, T., Kauffman, J., & Prisley, S. (2017). Lidar-based estimates of aboveground biomass in the continental US and Mexico using ground, airborne, and satellite observations. *Remote Sensing of Environment*, *188*, 127–140. https://doi.org/10.1016/j.rse.2016.10.038

Paolini, L., Grings, F., Sobrino, J. A., Jiménez-Muñoz, J. C., & Karszenbaum, H. (2006). Radiometric correction effects in landsat multi-date/multi-sensor change detection studies. *International Journal of Remote Sensing*, *27*(4), 685–704. https://doi.org/10.1080/01431160500183057

Proisy, C., Couteron, P., & Fromard, F. (2007). Predicting and mapping mangrove biomass from canopy grain analysis using Fourier based textural ordination of Ikonos images. *Remote Sensing of Environment*, *109*(3), 379–392. https://doi.org/10.1016/j.rse.2007.01.009

Reyes, H. H., Galarza, R. E., Torres, D. E. G., Sahagún, S. F. J., & de Nova, V. J. A. (2016). *Proyecto de fortalecimiento de las acciones de restauración del bosque de niebla en la RPC Xilitla. Programa de conservación de especies en riesgo (PROCER) 2016 Región noreste y Sierra Madre Oriental* [Project to strengthen cloud forest restoration actions in the Xilitla PRC. Conservation Program for Species at Risk (PROCER) 2016 Northeast Region and Sierra Madre Oriental]. Comisión Nacional de Áreas Naturales Protegidas.

Ruiz, D. C., Rodríguez, O. G., Leyva, L. J. C., & Enríquez, V. J. R. (2014). Metodologías Para estimar biomasa y carbono en especies forestales de méxico [Methodologies to estimate biomass and carbon in forest species in Mexico]. *Naturaleza y Desarrollo*, *12*(1), 28–45.

Sexton, J. O., Song, X. P., Feng, M., Noojipady, P., Anand, A., Huang, C., Kim, D., Collins, K. M., Channan, S., DiMiceli, C., & Townshend, J. R. (2013). Global, 30-m resolution continuous fields of tree cover: Landsat-based rescaling of MODIS vegetation continuous fields with LiDAR-based estimates of error. *International Journal of Digital Earth*, *6*(5), 427–448. https://doi.org/10.1080/17538947.2013.786146

Sherman, R. E., Fahey, T. J., Martin, P. H., & Battles, J. J. (2012). Patterns of growth, recruitment, mortality and biomass across an altitudinal gradient in a neotropical Montane forest, Dominican Republic. *Journal of Tropical Ecology*, *28*(5), 483–495. https://doi.org/10.1017/S0266467412000478

Spracklen, D. V., & Righelato, R. (2016). Carbon storage and sequestration of re-growing Montane forests in Southern Ecuador. *Forest Ecology and Management*, *364*, 139–144. https://doi.org/10.1016/j.foreco.2016.01.001

Sun, Z., Fang, H., Deng, M., Chen, A., Yue, P., & Di, L. (2015). Regular shape similarity index: A novel index for accurate extraction of regular objects from remote sensing images. *IEEE Transactions on Geoscience and Remote Sensing*, *53*(7), 3737–3748. https://doi.org/10.1109/TGRS.2014.2382566

Teferi, E., Uhlenbrook, S., Bewket, W., Wenninger, J., & Simane, B. (2010). The use of remote sensing to quantify wetland loss in the choke mountain range, upper Blue Nile basin. *Hydrology and Earth System Sciences*, *14*(12), 2415–2428. https://doi.org/10.5194/hess-14-2415-2010

Thomas, N., Simard, M., Castañeda-Moya, E., Byrd, K., Windham-Myers, L., Bevington, A., & Twilley, R. R. (2019). High-resolution mapping of biomass and distribution of marsh and forested wetlands in southeastern coastal Louisiana. *International Journal of Applied Earth Observation and Geoinformation*, *80*, 257–267. https://doi.org/10.1016/j.jag.2019.03.013

Torres, J. F., Flores, G. A., Calvo, F., Balam, L., Sepúlveda, V., García, I. E., Aguado, O., & Araujo, Z. (2010). *Valoración económica de seis Áreas Naturales Protegidas como sumideros de CO₂: Laguna Madre, Marismas Nacionales, Zicuirán-Infernillo, Sierra de Abra Tanchipa, Xilitla y Sierra Madre Oriental* [Economic valuation of six protected natural areas as CO2 sinks: Laguna Madre, Marismas Nacionales, Zicuirán-Infernillo, Sierra de Abra

Tanchipa, Xilitla and Sierra Madre Oriental] (137 p.). GTZ-CONANP. https://bit.ly/3fG84oj

Vanclay, J. K. (1994). *Modelling forest growth and yield: Applications to mixed tropical forests*. CAB International.

Vanclay, J. K. (1995). Growth models for tropical forests: A synthesis of models and methods. *Forest Science*, *41*(1), 7–42.

Watson, R. T., Noble, I. R., Bolin, B., Ravindranath, N. H., Verardo, D. J., & Dokken, D. J. (2000). *IPCC special report on land use land-use change and forestry*. IPCC.

Xu, L., Saatchi, S. S., Yang, Y., Yu, Y., & White, L. (2016). Performance of non-parametric algorithms for spatial mapping of tropical forest structure. *Carbon Balance and Management*, *11*(1), 18. https://doi.org/10.1186/s13021-016-0062-9

Young, N. E., Anderson, R. S., Chignell, S. M., Vorster, A. G., Lawrence, R., & Evangelista, P. H. (2017). A survival guide to landsat preprocessing. *Ecology*, *98*(4), 920–932. https://doi.org/10.1002/ecy.1730

Zhang, Y., Li, X., Ling, F., Atkinson, P. M., Ge, Y., Shi, L., & Du, Y. (2017). Updating landsat-based Forest cover maps with MODIS images using multiscale spectral-spatial-temporal superresolution mapping. *International Journal of Applied Earth Observation and Geoinformation*, *63*, 129–142. https://doi.org/10.1016/j.jag.2017.07.017